

PHOTON BUBBLES IN YOUNG MASSIVE STARS

N. J. Turner,¹ H. W. Yorke,¹ A. Socrates,² and O. M. Blaes²

RESUMEN

ABSTRACT

Spectroscopic studies indicate that gas in the photospheres of young O stars moves at speeds up to the sound speed. We show, using two-dimensional radiation MHD calculations and results from a local linear analysis, that the motions may be due to photon bubble instability if young O stars have magnetic fields.

Key Words: STARS: EARLY-TYPE — STARS: FORMATION

1. INTRODUCTION

Young high-mass stars may trigger or terminate nearby star and planet formation through ionizing radiation and winds launched from their surfaces. The properties of the radiation and winds depend on the structure of the stellar surface layers. Stars of more than 15 Solar masses reach the main sequence while still accreting material (Yorke & Sonnhalter 2002). High-mass main sequence stars are thought to have stably stratified outer layers, yet gas motions are present in the atmospheres of these stars.

Absorption lines formed in the photospheres of O stars are broader than expected based on the temperature, pressure and stellar rotation. If the rotation axes are randomly oriented with respect to our line of sight, some stars will be viewed pole-on and show no rotational broadening. However samples of O stars appear to contain no such pole-on cases (Slettebak 1956; Conti & Ebbets 1977; Penny 1996; Howarth et al. 1997). The minimum apparent equatorial rotation speed is a function of spectral type and luminosity. Among main-sequence O stars in the Small Magellanic Cloud cluster NGC 346, the excess broadening of UV metal lines ranges from 25 km s⁻¹ at O2, similar to the speed of sound at the photosphere, to 5 km s⁻¹ at O9.5 (Bouret et al. 2003).

Processes that might be responsible for the additional line broadening include

1. *Vertical velocity gradients in the stellar wind acceleration region* (Kudritzki 1992): Minimum line widths are similar in stars with and without strong outflows. Also, stellar atmosphere plus wind calculations including a variation in velocity through the acceleration region produce pho-

spheric lines similar to those in hydrostatic calculations (Bouret et al. 2003).

2. *Global non-radial pulsations*: Low levels of spectral line shape variations in main-sequence O stars (Fullerton et al. 1996) suggest that any global non-radial modes are either of low amplitude or high order. An unresolved issue is how such modes might be excited.
3. *Strange modes*: Instability occurs only for masses greater than 80 M_⊙ in zero-age main sequence stars with metallicity $Z = 0.02$ (Glatzel & Kiriakidis 1993), while excess photospheric line widths are observed in main-sequence stars with masses down to 20 M_⊙.
4. *Shaviv modes*: The instabilities are found only at luminosities greater than half the Eddington value (Shaviv 2001), while excess line broadening occurs in stars with one-tenth the Eddington luminosity.

Here we explore the possibility that a fifth mechanism, photon bubble instability (Arons 1992; Gammie 1998), may lead to small-scale motions in the surface layers of O stars. A general local WKB analysis of linear disturbances in optically-thick radiating atmospheres indicates instability under a wide range of conditions (Blaes & Socrates 2003). Photon bubbles are driven by the radiative flux (Figure 1), and grow if (1) Rosseland mean optical depth per wavelength is greater than unity, (2) a magnetic field is present, and (3) the radiative flux exceeds a critical value that in radiation-supported atmospheres is approximately the gas sound speed times the sum of gas and photon energy densities. The surface layers of O stars generally satisfy the first and third criteria, but until recently were thought to be unmagnetized. However θ^1 Ori C, the illuminating star of the Orion

¹Jet Propulsion Laboratory, California Institute of Technology.

²University of California at Santa Barbara.

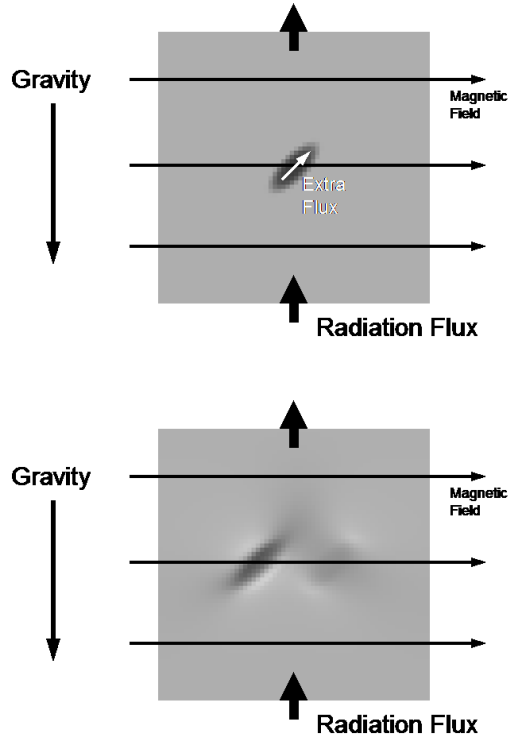


Fig. 1. How photon bubbles work. *Top*: A patch of atmosphere (gray square) is initially in hydrostatic balance. When density is reduced slightly in a small elongated region, photons diffuse more easily up the long axis. The perturbed radiation flux exerts an extra force with a component along the magnetic field. Gas is driven along the field to the right, out of the region of low density, and the perturbation grows. *Bottom*: As fresh gas enters the region of low density from the left, the pattern propagates to the left at about the gas sound speed.

Nebula and one of the nearest young O stars, shows polarimetric variations in photospheric lines with rotational phase, consistent with a 1.1 kG dipole field inclined 42° from the rotation axis (Donati et al. 2002). Also, narrow X-ray emission lines indicate some gas near the star moves more slowly than the wind. The line ratios show that most of the X-ray flux is thermal emission from plasma hotter than 15 million K, too hot to arise in shocks in the wind, and as hot as coronae in some magnetically active lower-mass stars (Schulz et al. 2003). Overall, there is good evidence for a magnetic field in θ^1 Ori C.

Photon bubbles, unlike strange modes, can grow in scattering atmospheres. They differ from Shaviv instabilities in that they require magnetic fields and may grow when the luminosity is substantially less than the Eddington value.

2. METHODS

A small patch of the surface layers of the star is followed in Cartesian coordinates (x, y, z) . The x -axis is horizontal, the z -axis vertical, and symmetry is assumed along the y -axis. The domain is 10^{10} cm on a side, or about 1.5% of the radius of θ^1 Ori C, and divided into 32×32 zones. The top of the domain is placed at the photosphere. The side boundaries are periodic, and the upper and lower boundaries are transparent walls through which radiation may pass, but gas and magnetic fields do not. The temperature of the lower boundary is fixed at its initial value, while the radiative flux is continuous across the upper boundary. The equations of radiation MHD,

$$\frac{D\rho}{Dt} + \rho \nabla \cdot \mathbf{v} = 0, \quad (1)$$

$$\rho \frac{D\mathbf{v}}{Dt} = -\nabla p + \frac{1}{4\pi} (\nabla \times \mathbf{B}) \times \mathbf{B} + \frac{\chi_F \rho}{c} \mathbf{F} - \rho g \hat{\mathbf{z}}, \quad (2)$$

$$\rho \frac{D}{Dt} \left(\frac{e}{\rho} \right) = -p \nabla \cdot \mathbf{v} - \kappa_P \rho (4\pi B - cE), \quad (3)$$

$$\rho \frac{D}{Dt} \left(\frac{E}{\rho} \right) = -\nabla \cdot \mathbf{F} - \nabla \mathbf{v} : \mathbf{P} + \kappa_P \rho (4\pi B - cE), \quad (4)$$

and

$$\frac{\partial \mathbf{B}}{\partial t} = \nabla \times (\mathbf{v} \times \mathbf{B}), \quad (5)$$

(Mihalas & Mihalas 1984; Stone, Mihalas & Norman 1992; Blaes & Socrates 2003) are solved using the ZEUS code (Stone & Norman 1992a,b) with its flux-limited radiation diffusion module (Turner & Stone 2001). A uniform gravity g is included. Rotation is ignored, as photon bubbles grow to saturation within a typical stellar rotation period. Emission proportional to the blackbody rate B is assumed in equations 3 and 4. Temperatures are calculated using a mean mass per particle of 0.6 protons. The total flux-mean opacity χ_F includes contributions from electron scattering $0.34 \text{ cm}^2 \text{ g}^{-1}$ and bound-free and free-free processes $2 \times 10^{52} \rho^{4.5} e^{-3.5} \text{ cm}^2 \text{ g}^{-1}$, where e is the gas internal energy per unit volume and ρ is the mass density. The Planck-mean absorption opacity κ_P due to the bound-free and free-free effects is $7.4 \times 10^{53} \rho^{4.5} e^{-3.5} \text{ cm}^2 \text{ g}^{-1}$. The radiative flux $\mathbf{F} = -\frac{c\Lambda}{\chi_F \rho} \nabla E$ is calculated using a limiter Λ that equals $\frac{1}{3}$ in optically-thick regions, and is reduced in regions of low optical depth so that the flux does not exceed the product of the radiation energy density E and light speed c (Levermore & Pomraning 1981). The set of equations is closed using an ideal gas equation of state $p = (\gamma - 1)e$ with $\gamma = 5/3$.

Initial conditions are constructed by integrating the equations of hydrostatic equilibrium and radiative flux conservation from the photosphere down into the interior. Three initial states are considered, spanning the range of effective temperatures found in O stars. The photospheric temperatures in Kelvins and densities in g cm^{-3} are (A) 50 000, 1.8×10^{-9} , (B) 40 000, 2.2×10^{-9} , and (C) 30 000, 3.0×10^{-9} . Surface gravity $10^{3.8} \text{ cm s}^{-2}$ is used in all cases. The Eddington ratios between the last two terms in equation 2 at the photospheres are (A) 0.65, (B) 0.28, and (C) 0.11. We study the growth of photon bubbles at the stellar magnetic equator by beginning with a uniform, horizontal magnetic field of 1 kG. Radiation, gas and magnetic pressures at the photosphere are in ratios (A) 0.40 : 0.31 : 1, (B) 0.16 : 0.31 : 1, and (C) 0.05 : 0.31 : 1. Random zone-to-zone initial density perturbations with amplitude 0.1% are added only in the middle half of the domain height, to reduce any effects of the boundaries on the linear growth.

3. RESULTS

Each calculation passes through three stages. First, the perturbations cause small damped vertical oscillations with period equal to the gas sound crossing time and amplitude 0.1 km s^{-1} . Next, linear eigenmodes appear and grow exponentially. The fastest-growing modes are gas sound waves with wavefronts inclined 30 to 45 degrees from vertical, and group velocity roughly parallel to the magnetic field. Finally, the growth saturates and amplitudes vary little over many gas sound crossing times.

3.1. Linear Growth

The time histories of the horizontal kinetic energies are shown in Figure 2. Linear growth rates increase with photospheric temperature. In the 50 000 K case (A), the fastest mode has 3 wavelengths in the domain width and 2 in the height, corresponding to wavelength $2.8 \times 10^9 \text{ cm}$ and wavevector 34° from horizontal. The power in the mode, measured using the Fourier transform of the horizontal velocity pattern, grows e -fold every 3000 seconds. The growth rate is $2/3$ that obtained by solving the linear dispersion relation, Blaes & Socrates (2003) equation 49, for conditions at the center of the computational domain. The slower growth in the simulation may be due to the modest grid resolution.

3.2. Saturation

The disturbances reach larger amplitudes in the cases with hotter photospheres. The largest horizontal velocities are 30 km s^{-1} in the 50 000 K case (A),

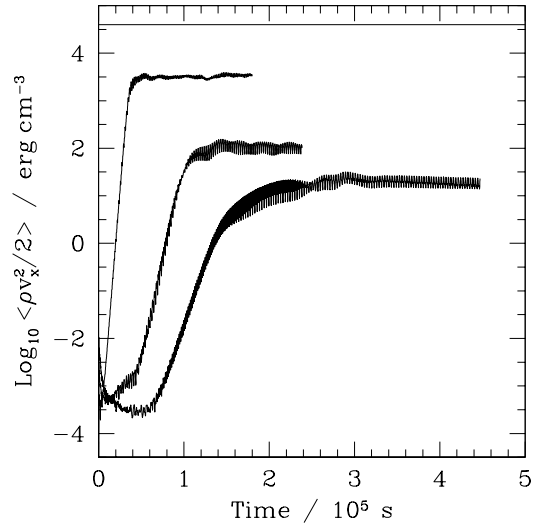


Fig. 2. Domain-averaged kinetic energies in horizontal motions versus time, in the calculations with photospheric temperatures 50 000 (top), 40 000 (middle), and 30 000 K (bottom). The upper horizontal line indicates the energy density in the initial magnetic field.

12 km s^{-1} in the 40 000 K case (B), and 6 km s^{-1} in the 30 000 K case (C). In the hottest case (A), the speeds are similar to the isothermal gas sound speed of 26 km s^{-1} at the photosphere, and weak shocks are present. The structure resembles that proposed by Begelman (2001), but with crossed shocks due to the initial horizontal symmetry. Gas oscillates back and forth along magnetic field lines, experiencing repeated compression and expansion. Densities vary about their initial values by up to a factor three, while radiation energy remains almost uniform due to rapid diffusion (Figure 3). Radiation escapes more easily through the inhomogeneous atmosphere than through the original hydrostatic structure, and the time-averaged radiative flux is 10% greater than initially. The density variations in the 40 000 K case (B) are 50%, and in the 30 000 K case (C) are 20%. The magnetic fields bend 30° up and down in the hottest case, and remain close to horizontal in the two cooler cases.

4. CONCLUSIONS

Photon bubble instability is present in the surface layers of magnetized main-sequence O stars according to the results of a local linear WKB analysis. We use two-dimensional radiation MHD calculations with horizontal magnetic fields and closed vertical boundaries to show that the instability can lead to small-scale movements of gas in the surface layers, with velocities about equal to the

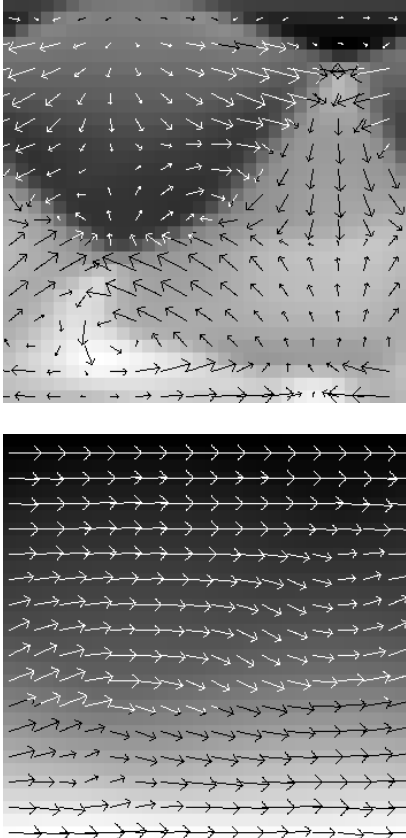


Fig. 3. Snapshot of saturated photon bubble instability in the calculation with photospheric temperature 50 000 K, at 56 000 seconds. The initial photosphere lies along the top boundary, and the domain height and width are 10^{10} cm. *Top*: Density on a gray scale logarithmic between 1.2×10^{-9} (black) and 1.3×10^{-8} g cm^{-3} (white). Velocities are shown by arrows, the longest corresponding to 29 km s^{-1} . *Bottom*: Radiation pressure on a gray scale linear between 6 600 and 210 000 dyn cm^{-2} . Magnetic fields are shown by arrows, the longest 1500 G.

observed linewidth excesses. In a calculation with parameters appropriate for an early O star, photon bubbles result in horizontal density variations near the photosphere. Radiation diffuses more rapidly through the inhomogeneities than through the hydrostatic atmosphere with the same column depth, and the radiative flux is 10% greater than that calculated assuming hydrostatic equilibrium. An enhanced flux may affect measurements of stellar parameters. Issues remaining to be resolved

include the dependence on the local magnetic field orientation and the shapes of the spectral lines expected from emission integrated over the stellar disk.

Photon bubbles reaching amplitudes similar to those in the hottest case we considered may eject blobs of gas through the photosphere, and could lead to density variations in the winds of O stars. The motions might transfer energy into an initially weak magnetic field. Additional radiation MHD calculations indicate the saturation amplitude generally increases with decreasing surface gravity, so photon bubbles may reach larger amplitudes in O giants and supergiants. Solutions of the dispersion relation show that photon bubbles may be present also in accretion disks around young massive stars.

N. J. T. was supported by a National Research Council fellowship. The work was carried out in part at the Jet Propulsion Laboratory, California Institute of Technology.

REFERENCES

- Arons J. 1992, *ApJ*, 388, 561
 Begelman M. C. 2001, *ApJ*, 551, 897
 Blaes O. & Socrates A. 2003, *ApJ*, 596, 509
 Bouret J.-C. et al. 2003, *ApJ*, 595, 1182
 Conti P. S. & Ebbets D. 1977, *ApJ*, 213, 438
 Donati J.-F., Babel J., Harries T. J., Howarth I. D., Petit P. & Semel, M. 2002, *MNRAS*, 333, 55
 Fullerton A. W., Gies D. R. & Bolton C. T. 1996, *ApJS*, 103, 475
 Gammie C. 1998, *MNRAS*, 297, 929
 Glatzel W. & Kiriakidis M. 1993, *MNRAS*, 262, 85
 Howarth I. D., Seibert K. W., Hussain G. A. J. & Prinja R. K. 1997, *MNRAS*, 284, 265
 Kudritzki R. P. 1992, *A&A*, 266, 395
 Levermore C. D. & Pomraning G. C. 1981, *ApJ*, 248, 321
 Mihalas D., & Mihalas B. W. 1984, *Foundations of Radiation Hydrodynamics* (Oxford: Oxford Univ. Press)
 Penny L. R. 1996, *ApJ*, 463, 737
 Schulz N. S., Canizares C., Huenemoerder D., & Tibbets K. 2003, *ApJ*, 595, 365
 Shaviv N. J. 2001, *ApJ*, 549, 1093
 Slettebak A. 1956, *ApJ*, 124, 173
 Stone J. M., & Norman M. L. 1992a, *ApJS*, 80, 753
 Stone J. M., & Norman M. L. 1992b, *ApJS*, 80, 791
 Stone J. M., Mihalas D., & Norman M. L. 1992, *ApJS*, 80, 819
 Turner N. J. & Stone J. M. 2001, *ApJS*, 135, 95
 Yorke H. W. & Sonnhalter C. 2002, *ApJ*, 569, 846

N. J. Turner and H. W. Yorke: MS 169-506, Jet Propulsion Laboratory, California Institute of Technology, Pasadena CA 91109, USA; neal.turner@jpl.nasa.gov.

O. M. Blaes and A. Socrates: Physics Department, University of California, Santa Barbara CA 93106, USA.